

Online Automated Generation of an Aortic Model for MR Guided Interventions

N. Karlsson¹, K. J. Kirchberg², L. Pan¹, A. J. Flammang¹, C. H. Lorenz¹, and W. Gilson¹

¹Center for Applied Medical Imaging, Siemens Corporation, Corporate Research, Baltimore, MD, United States, ²Center for Applied Medical Imaging, Siemens Corporation, Corporate Research, Princeton, NJ, United States

Introduction: Virtual endoscopy refers to a method of processing 3D image data to generate visualizations that simulate views commonly achieved with conventional endoscopes. These visualizations exploit the detailed image information achieved from such imaging modalities as computed tomography and MRI, and have been used in lieu of conventional endoscopy procedures to avoid the associated risks. Virtual endoscopy has been used in a variety of anatomical regions including the colon, carotid arteries, brain, parenchyma and aorta. Classically, generation of the virtual endoscope renderings is performed following complete acquisition of 3D image data.

Recently, a new strategy for generating virtual endoscopic views of the aorta in real-time was introduced using interactive, segmentation-based modeling and rendering [1]. This method was designed in the context of interventional MRI with the goal of aiding the physician during aortic interventions, e.g. stent placement. It has also been used to measure pulse wave velocity [2]. For generation of a 4D model, real-time 2D MR images at arbitrary orientations about the aorta are acquired continuously with real-time segmentation to build and optimize the model.

In this study, real-time MR virtual endoscopy has been extended to include additional optimization for improved 4D modeling. Furthermore, a validation of online 4D model generation was performed in a healthy subject.

Methods: Prototype Design. The virtual endoscopy prototype is implemented as a module in the Interactive Front End (IFE) navigation software [3]. IFE interfaces with a real-time interactive pulse sequence (BEAT_IRTTT) to provide advanced visualization and scanner control for interventional MRI procedures. For this study, the aorta is modeled as a generalized cylinder and is formed by first semi-automatically segmenting four aortic cross-sections at different locations along the vessel, namely 1) distal descending aorta, 2) proximal descending/proximal ascending aorta, and 3) the apex of the aortic arch. An initial tubular model is then fitted to the 4 points. Subsequently, additional images of arbitrary positions and orientations are added to update the 3D model. Regions of interest, automatically determined by the current model, are extracted and stored for each new image. Based on a constantly updated global intensity distribution model the image pixels are classified as belonging to the inside or the outside of the vessel. The 3D model is continuously updated to best match all the acquired data points. This is achieved by cost function modeling a variation of the Mumford-Shah energy term [4]. The reduction to a relatively simple shape model (circular tube) allows interpolation of the 3D model in areas where no or only sparse image data is available. Cardiac motion is taken into account by optimizing a deformation for each of a number of discrete cardiac phases (10 phases were used in this study).

In Vivo Testing and Validation. To evaluate the prototype performance, a healthy volunteer was imaged using a 1.5T scanner (MAGNETOM Avanto, Siemens Healthcare, Erlangen, Germany). The BEAT_IRTTT sequence was used to acquire images, while the volunteer breathed shallowly, using an SSFP acquisition (TE 1.7ms, TR 3.4ms, 2.3x2.3x8mm resolution, flip angle 60°) with slices oriented (1) transverse and (2) parallel to the aortic length (i.e. “candy cane view”). Though ungated, the sequence recorded the time between each image acquisition and its preceding ECG trigger to be used for retrospective binning. A total of 100 measurements per transverse slice location were acquired covering 80 mm in 10 mm intervals of the aorta extending from above the arch to just distal to the heart apex. Similarly, slices oriented with and orthogonal to the long-axis candy cane view were acquired.

In the same study, breath-hold, retrospectively-gated, segmented cine SSFP images were acquired (TE 1.4ms, TR 3.2ms, 1.3x1.3x8.0mm resolution, 11 segments, 25 cardiac phases) for comparison to the model. A total of 7 slices with a 12mm gap were collected. In addition, one cine slice was acquired orthogonal to the top of the aortic arch. Temporal resolution of the collected slices was 261 ms per frame.

Data Analysis. The aorta was semi-automatically segmented for seven slices and all cardiac phases (Argus, Siemens Healthcare, Erlangen, Germany) of the cine data set. A custom-built MATLAB (MathWorks, Natick, MA) program was used to create binary images from the segmented images and compute the center of mass (CoM) of each segment. A morphological ‘remove’ operation was performed to detect the edges of the segments. The mean radius for each segment was approximated by averaging the Euclidean distances from the CoM to each edge point. The slice location and orientation for each cine slice was collected and used to extract the corresponding radius and centerline location in the 4D model. Radii for each slice location over time were compared.

Results: The real-time MR virtual endoscopy successfully generated a 4D model of a healthy human aorta (Fig.1). A shift (9.8mm) in location of the centerline/CoM between the model and the cine data was observed and was likely associated with respiratory motion. However, the radii at each slice location demonstrated mean errors (averaged over time steps) ranging from 0.31 – 1.52mm, which is less than the real-time image resolution (Fig. 2).

Discussion: Real-time virtual MR is feasible and may be potentially useful for monitoring aortic geometry and contractility during interventional MRI procedures. More extensive validation is needed to evaluate the prototype performance in diseased aortas. The concept can also be extended to provide real-time updates of other target organs.

References

1. Kirchberg KJ, et al. ISMRM (2006): 268.
2. Kirchberg KJ, et al. ISMRM (2007): 5984.
3. Lorenz CH et al. ISMRM (2005); 2170.
4. Mumford D, Commun. Pure Appl. Math, 1989;42:577–685, 1989

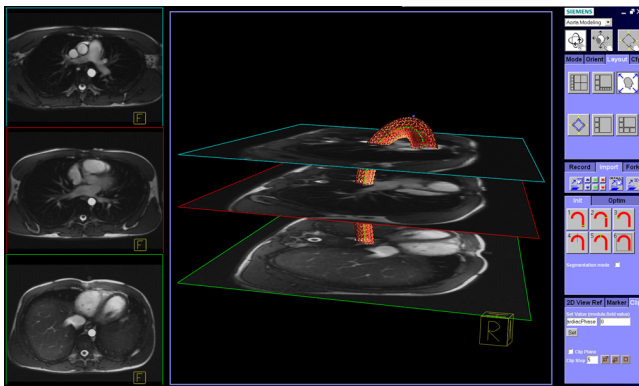


Fig 1. The real-time virtual endoscope integrated into the IFE navigation prototype. A 3D model of the aorta is shown as a red mesh with a green centerline. Example cine images from three of the 8 slice locations used for validation are overlaid on the model.

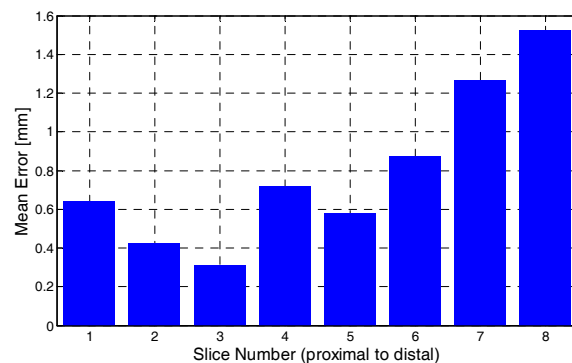


Fig. 2. Mean error of estimated radius of the aorta at 8 slice positions. The slices are ordered from proximal (aortic arch) to distal.